

LEVEL

12

AD A 071 896

Global Lightning Distribution at Dawn and Dusk for August-December 1977 as Observed by the DMSP Lightning Detector

B. C. EDGAR
Space Sciences Laboratory
Laboratory Operations
The Aerospace Corporation
El Segundo, Calif. 90245

15 June 1979

Interim Report

APPROVED FOR PUBLIC RELEASE;
DISTRIBUTION UNLIMITED

Prepared for

AIR FORCE TECHNICAL APPLICATIONS CENTER
Patrick Air Force Base, Fla. 32935

SPACE AND MISSILE SYSTEMS ORGANIZATION
AIR FORCE SYSTEMS COMMAND
Los Angeles Air Force Station
P.O. Box 92960, Worldway Postal Center
Los Angeles, Calif. 90009

DDIC
JUL 27 1979

DDC FILE COPY

79 07 27 004

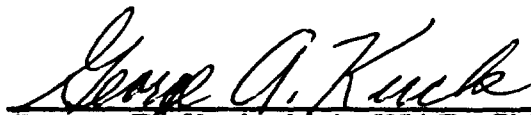
This interim report was submitted by The Aerospace Corporation, El Segundo, CA 90245, under Contract No. F04701-78-C-0079 with the Space and Missile Systems Organization, Deputy for Advanced Space Programs, P.O. Box 92960, Worldway Postal Center, Los Angeles, CA 90009. It was reviewed and approved for The Aerospace Corporation by G. A. Paulikas, Director, Space Sciences Laboratory. Lieutenant A. G. Fernandez, SAMSO/YCPT, was the project officer for Advanced Space Programs.

This report has been reviewed by the Information Office (OI) and is releasable to the National Technical Information Service (NTIS). At NTIS, it will be available to the general public, including foreign nations.

This technical report has been reviewed and is approved for publication. Publication of this report does not constitute Air Force approval of the report's findings or conclusions. It is published only for the exchange and stimulation of ideas.



Arturo G. Fernandez, Lt, USAF
Project Officer



George E. Kuck, Maj, USAF, Chief
Technology Plans Division

FOR THE COMMANDER



FLOYD R. STUART, Colonel, USAF
Asst. Deputy for Technology

UNCLASSIFIED

SECURITY CLASSIFICATION OF THIS PAGE (When Data Entered)

REPORT DOCUMENTATION PAGE		READ INSTRUCTIONS BEFORE COMPLETING FORM
1. REPORT NUMBER 18 SAMSO-TR-79-43	2. GOVT ACCESSION NO.	3. RECIPIENT'S CATALOG NUMBER
4. TITLE (and Subtitle) GLOBAL LIGHTNING DISTRIBUTION AT DAWN AND DUSK FOR AUGUST-DECEMBER 1977 AS OBSERVED BY THE DMSP LIGHTNING DETECTOR		5. TYPE OF REPORT & PERIOD COVERED Interim
6. AUTHOR(s) 10 Bruce C. Edgar		7. PERFORMING ORG. REPORT NUMBER 14 TR-0079(4639)-1
8. PERFORMING ORGANIZATION NAME AND ADDRESS The Aerospace Corporation El Segundo, Calif. 90245		9. CONTRACT OR GRANT NUMBER(s) 15 F04701-78-C-0079
10. CONTROLLING OFFICE NAME AND ADDRESS Air Force Technical Applications Center Patrick Air Force Base, Fla. 32935		11. PROGRAM ELEMENT, PROJECT, TASK AREA & WORK UNIT NUMBERS 12 REPORT DATE 15 Jun 1979
13. MONITORING AGENCY NAME & ADDRESS (if different from Controlling Office) Space and Missiles Systems Command Air Force Systems Command Los Angeles, Calif. 90009		14. NUMBER OF PAGES 33
15. DISTRIBUTION STATEMENT (of this Report) Approved for public release; distribution unlimited.		16. SECURITY CLASS. (of this report) Unclassified
17. DISTRIBUTION STATEMENT (of the abstract entered in Block 20, if different from Report)		18. DECLASSIFICATION/DOWNGRADING SCHEDULE
19. SUPPLEMENTARY NOTES Submitted for presentation at International Union of Radio Science, Helsinki, Finland, 1 August 1978.		
20. KEY WORDS (Continue on reverse side if necessary and identify by block number)		
21. ABSTRACT (Continue on reverse side if necessary and identify by block number) The lightning detector aboard a DMSP satellite in a dawn-dusk polar orbit sampled lightning activity worldwide during August-December 1977. At dawn the distribution of events is somewhat evenly spread over both hemispheres with a slight bias towards land areas in the summer hemisphere. There is significant activity over the oceans in both hemispheres at dawn, presumably due to radiative cooling of the atmosphere. However, at dusk lightning occurs primarily over the warmer land areas in the summer hemisphere with very		

DD FORM 1473
(FACSIMILE)

UNCLASSIFIED

SECURITY CLASSIFICATION OF THIS PAGE (When Data Entered)

UNCLASSIFIED

SECURITY CLASSIFICATION OF THIS PAGE(When Data Entered)

19. KEY WORDS (Continued)

20. ABSTRACT (Continued)

Cont. > few events in the winter hemisphere. Also there is a marked increase of lightning events about the tropical convergence zone. These distribution plots give for the first time a global snapshot of lightning activity which could lead to a better understanding of the global atmospheric noise distribution.

Accession For	
NTIS GRA&I	<input checked="checked" type="checkbox"/>
DDC TAB	<input type="checkbox"/>
Unannounced	<input type="checkbox"/>
Justification	<input type="checkbox"/>
By _____	
Distribution/	
Availability	
Dist	Available for special

UNCLASSIFIED

SECURITY CLASSIFICATION OF THIS PAGE(When Data Entered)

CONTENTS

INTRODUCTION	5
DESCRIPTION OF EXPERIMENT	7
GENERAL WAVEFORM STATISTICS	11
GEOGRAPHICAL DISTRIBUTION OF LIGHTING ACTIVITY	17
DISCUSSION	18
APPLICATIONS	30
CONCLUSIONS	32
REFERENCES	33

TABLES

1. Sensor Sampling and Trigger Modes	10
2. Total Lightning Counts	14
3. Global Occurrence Rates	29

FIGURES

1.	Schematic of the viewing area of the lightning detector	8
2.	Encounter with a localized lightning cell at 32°N	12
3a.	Typical power-time profiles for six events observed over the S.E. United States in August 1978	15
3b.	Distribution of peak optical power for two latitude regions: high latitude and equatorial	16
4.	Lightning distribution for the period August 2- September 10, 1977	19
5.	Lightning distribution for the period September 10- October 11, 1977	20
6.	Lightning distribution for the period November 6- December 2, 1977	21
7.	GOES-1 Satellite IR map of the cloud distribution for August 2, 1977	24
8.	GOES-1 Satellite IR map of the cloud distribution for October 4, 1977	25
9.	GOES-1 Satellite IR map of the cloud distribution for November 30, 1977	26
10.	Comparison of CCIR noise map for (a) June-August with the August lightning detector data and (b) September- November with the September-October satellite data	31

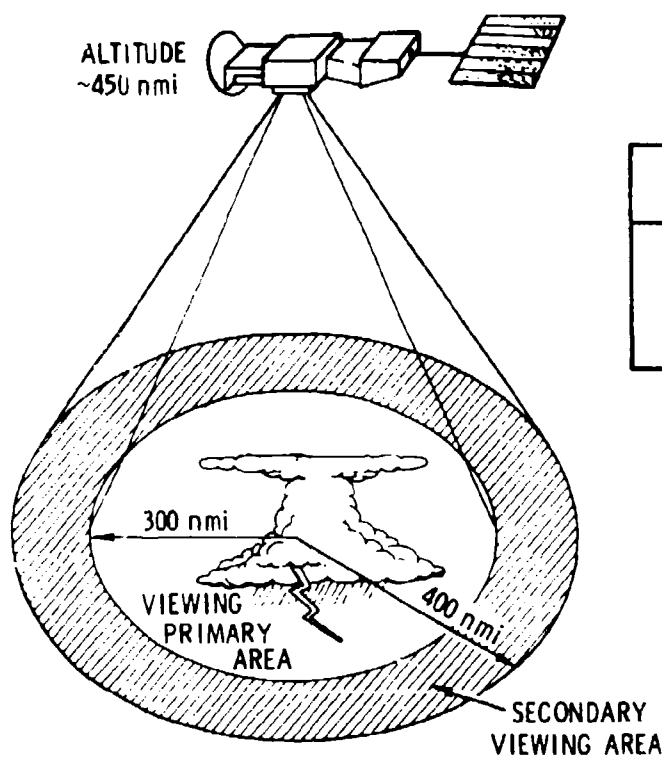
INTRODUCTION

Previous lightning measurements and analyses have been seriously restricted by the limited perspective inherent in ground-based observations. A truly global, continuously available perspective of lightning activity can be obtained most readily from satellite platforms. Such satellite data are now available as a result of a special lightning experiment now flying on Defense Meteorological Satellite Program (DMSP) Flight 2. This experiment was designed to detect and record optical pulse profiles from lightning flashes occurring below the spacecraft within a circle of 780 Km radius. The main objectives were to develop peak power and waveform statistics, and to map global distributions of lightning activity. A previous American Geophysical Union paper (Edgar and Turman, 1977) presented waveform statistics collected over the Southeast United States during the summer of 1977. The present paper will amplify these results and show worldwide distribution of lightning activity over the period August - December 1977.

DESCRIPTION OF EXPERIMENT

In June 1977, the Defense Meteorological Satellite Program (DMSP) Flight 2 weather satellite was launched into an 830 Km altitude, sun-synchronous (dawn-dusk) polar orbit. The primary sensors on the satellite provide visible and infrared (IR) pictures of the world's weather system. The PBE secondary sensor was designed and built by Sandia Laboratories, Albuquerque, to provide additional information concerning optical characteristics of lightning. The main optical sensor in the PBE is a silicon photodiode, with peak sensitivity at 0.9 micrometer. The conical field of view is directed vertically downward; the unvignetted half angle is 35° , and limited response, as a result of vignetting of the photodiode, is obtained out to 39.5° half angle. The angular response of the sensor is plotted in Figure 1. The projection of the vignetted field of view on the earth is a circle of 780 Km radius, centered at the satellite subpoint.

The data processing electronics include a feedback circuit to compensate for the DC component due to the earth's albedo, a threshold trigger circuit, and a lightning verification gate. DC compensation allows lightning detection at threshold even under full earth illumination. A number of false triggers, however, are sometimes generated by a sudden change in



DYNAMIC RANGE: 10^9 - 10^{13} watts

SAMPLE RATE	TIME RESOLUTION	MIN PULSE DURATION
62.4 kHz	16 μ sec	80 μ sec
31.2	32	160
15.6	64	320
7.8	128	640

DETECTOR: SILICON PHOTODIODE

$\lambda \sim 0.7$ - 1.0μ m

PRIMARY VIEWING AREA

$\sim 10^6 \text{ km}^2$

DAWN-DUSK ORBIT

Figure 1. Schematic of the viewing area of the lightning detector

the background illumination level, a situation which can arise as the sensor field of view moves over a wide band of high clouds being illuminated by the sun. These "compensation triggers" are easily recognized and have been eliminated from the lightning data base. When a lightning flash occurs within the sensor's field and the rapidly rising optical signal exceeds a predetermined amplitude threshold, digital sampling of the signal is begun. Any of the four sampling rates listed in Table 1 may be selected. The instantaneous optical power is sampled and digitized into 63 logarithmically spaced intervals between 4×10^9 and 10^{13} watts. A data frame of 30 samples is stored in a 32 event memory if the signal passes a lightning verification gate--basically a test of the pulse width. The verification requires that at least 5 of the first 8 samples have a digital amplitude greater than threshold, and was included in the trigger logics to eliminate triggers due to high energy particles.

Because of telemetry limitations, only one event frame is read from the event memory to the primary system tape recorder every four seconds. Event time is not registered until the event frame is placed on the primary tape recorder; event time can thus be measured with precision no greater than 4 seconds. Since event frame readout occurs at a rate much slower than the potential event triggering rate, it is possible that an event frame will be logged and timed as long as 128 seconds after its occurrence. An event trigger counter is provided to resolve this possible timing uncertainty.

To illustrate the lightning data obtained from this sensor, a typical example will be discussed. Figure 2 displays the visible cloud image taken with the DMSP prime sensors on 22 July 1977. The Great Lakes region is

TABLE 1
SENSOR SAMPLING AND TRIGGER MODES

<u>SAMPLE RATES</u>		
<u>System Sample Rate</u>	<u>Time Resolution</u>	<u>Minimum Pulse Duration*</u>
62.4 KHz	16 μ sec	80 μ sec
31.2	32	160
15.6	64	320
7.8	128	640

<u>TRIGGER LEVELS</u>	
<u>Digital Level</u>	<u>Source Power at Subpoint</u>
8	4×10^9 watts
12	9×10^9
16	1.8×10^{10}
24	6.5×10^{10}
32	3.2×10^{11}
40	9×10^{11}

* Required by Lightning Verification Gate

outlined in the upper left and the Mississippi River is in the upper central portion of the photograph. A stationary front lies across the states of Oklahoma, Arkansas, Mississippi, and Alabama, extending from 40° N, 100° W to 32° N, 80° W. The first lightning signal from this region was detected when the satellite subpoint was at 38.5° N latitude. The upper circle in Figure 2 is the field of view of the lightning sensor for this trigger. As the satellite continued its southward motion over the front the sensor collected a total of 17 lightning triggers. The last trigger in this sequence occurred with a satellite subpoint of 25.8° N; the lower circle in Figure 2 is the field of view at the time of the final trigger. This sequence of triggers suggests that the electrically active storm cells which generated the lightning activity were located along the southern portion of the front. Figure 2 also shows that the location error can be as much as 6° .

GENERAL WAVEFORM STATISTICS

The previous paper by Edgar and Turman (1977) presented statistics concerning lightning waveform properties. That analysis was based on a relatively small population of lightning data collected over the Southeast United States. Similar analysis of the larger population now available agrees well with those results; therefore, we need only to review those statistics now. Signal rise time was defined as the interval between the start time (above threshold) and the time when the signal peaks. The median rise time was 150 microseconds, and the longest rise time was about 600 microseconds. Pulse duration was defined as the total time that the signal remains above threshold. The frequency distribution of this

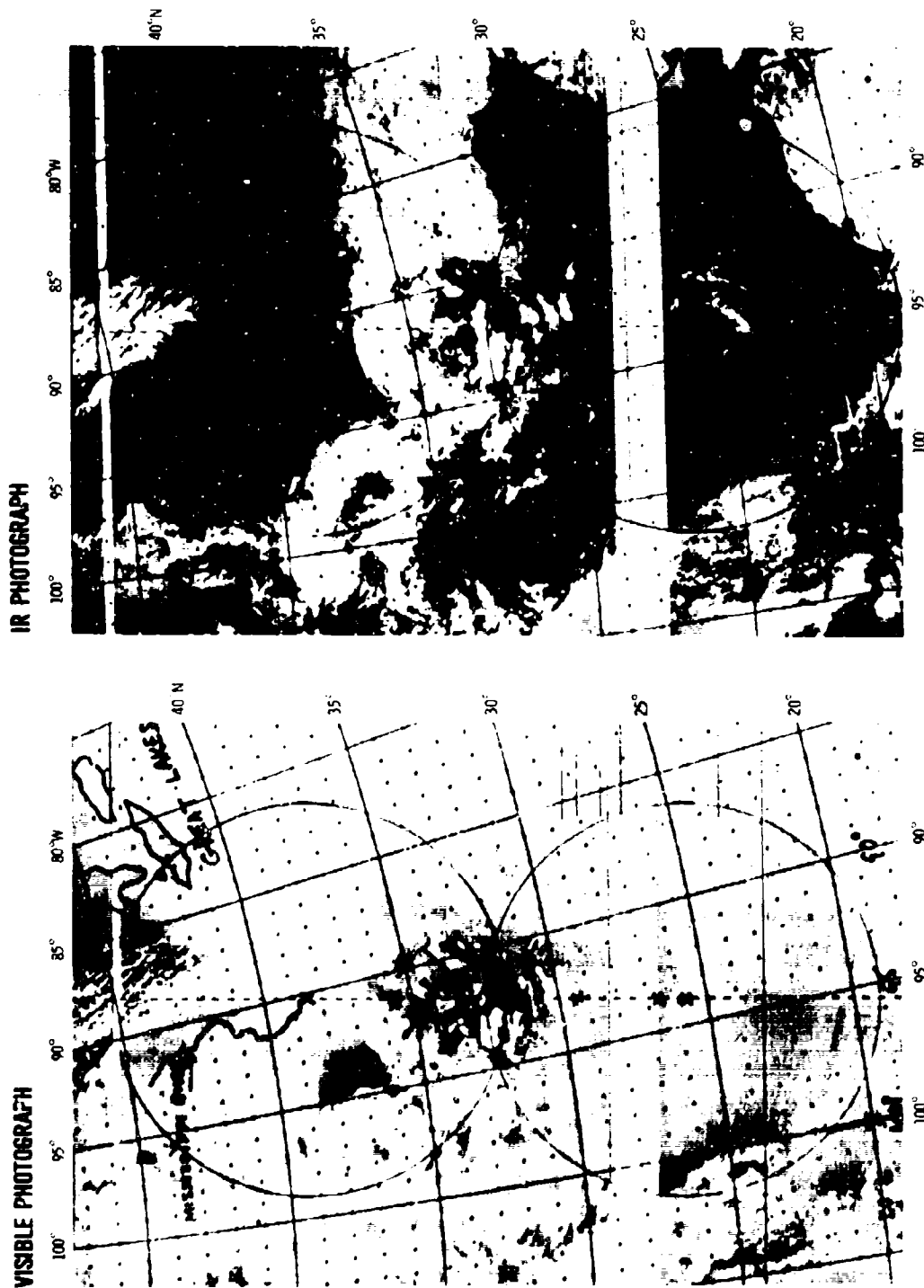


Figure 2. Encounter with a localized lightning cell at 32°N. The circles give the field of view for the first and last triggers and the overlap pinpoints the active region. The X's mark the subsatellite point at each trigger in time.

parameter is particularly important to understand, because of the minimum pulse duration requirement for triggering the sensor. As shown in Table 1, the slower system sampling rates imposed longer minimum pulse duration requirements, and thus short duration pulses would not be detected at the slower sampling rates. The median pulse duration was 400 microseconds, and the longest recorded pulses were less than 2 milliseconds in duration. Although it was not possible to detect lightning pulses shorter than 80 microseconds duration (sensor design limitation), this minimum duration requirement did not seem to unduly bias the pulse duration frequency statistics. Table 2 gives the fraction of lightning strokes detected, for each of the sampling rates.

Figure 3 shows the power-time profiles for 6 typical events. The rise times range from 100 to 150 microseconds, but the duration times show a wide variation. The events with < 0.5 millisecond duration times agree with the typical duration times of negative return strokes as photographed by Berger (1967) at Mt. San Salvatore. However the longer events (> 1.0 millisecond) may be due to positive upward strokes or cloud flashes since Berger (1967) shows examples of these events lasting up to 3 milliseconds. Only 7% of the satellite observed events had duration times greater than 1 millisecond which agrees with the percentage of positive strokes observed on the ground (Uman, 1969).

TABLE 2
Total Lightning Counts

	<u>Dawn</u>		<u>Dusk</u>	
	<u>Total</u>	<u>Per Min.</u>	<u>Total</u>	<u>Per Min.</u>
Aug-Sep	2460	0.2	3013	0.3
Sep-Oct	3871	0.3	2900	0.2
Nov	2605	0.2	1269	0.1

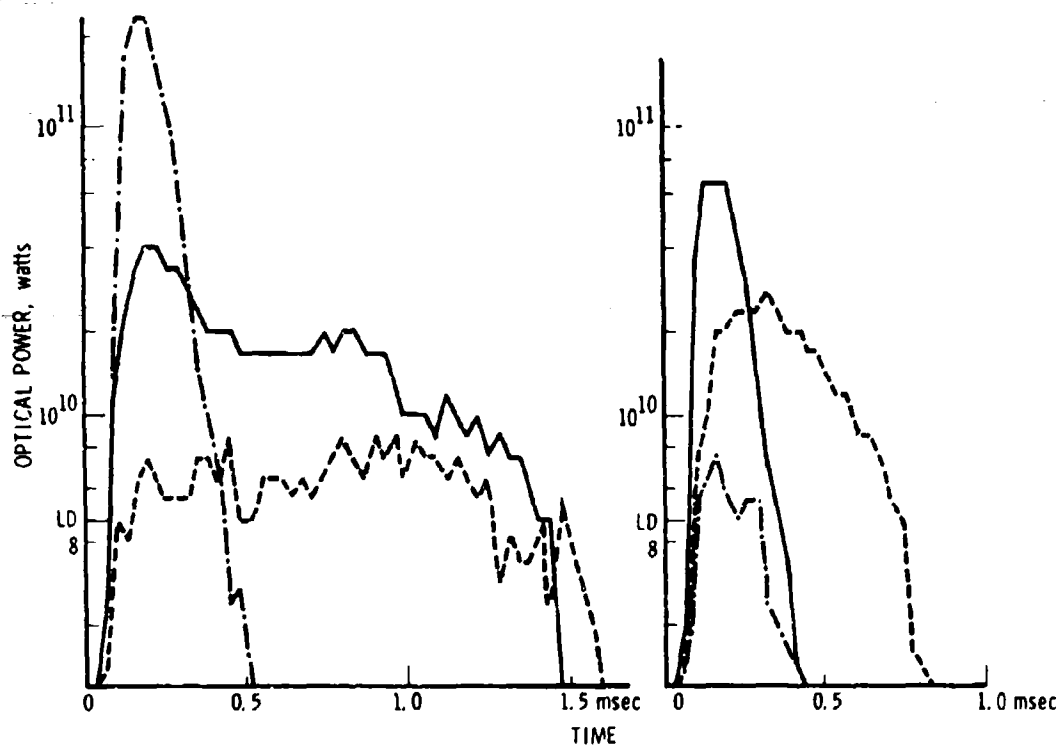


Figure 3a. Typical power-time profiles for six events observed over the S.E. United States in August 1978

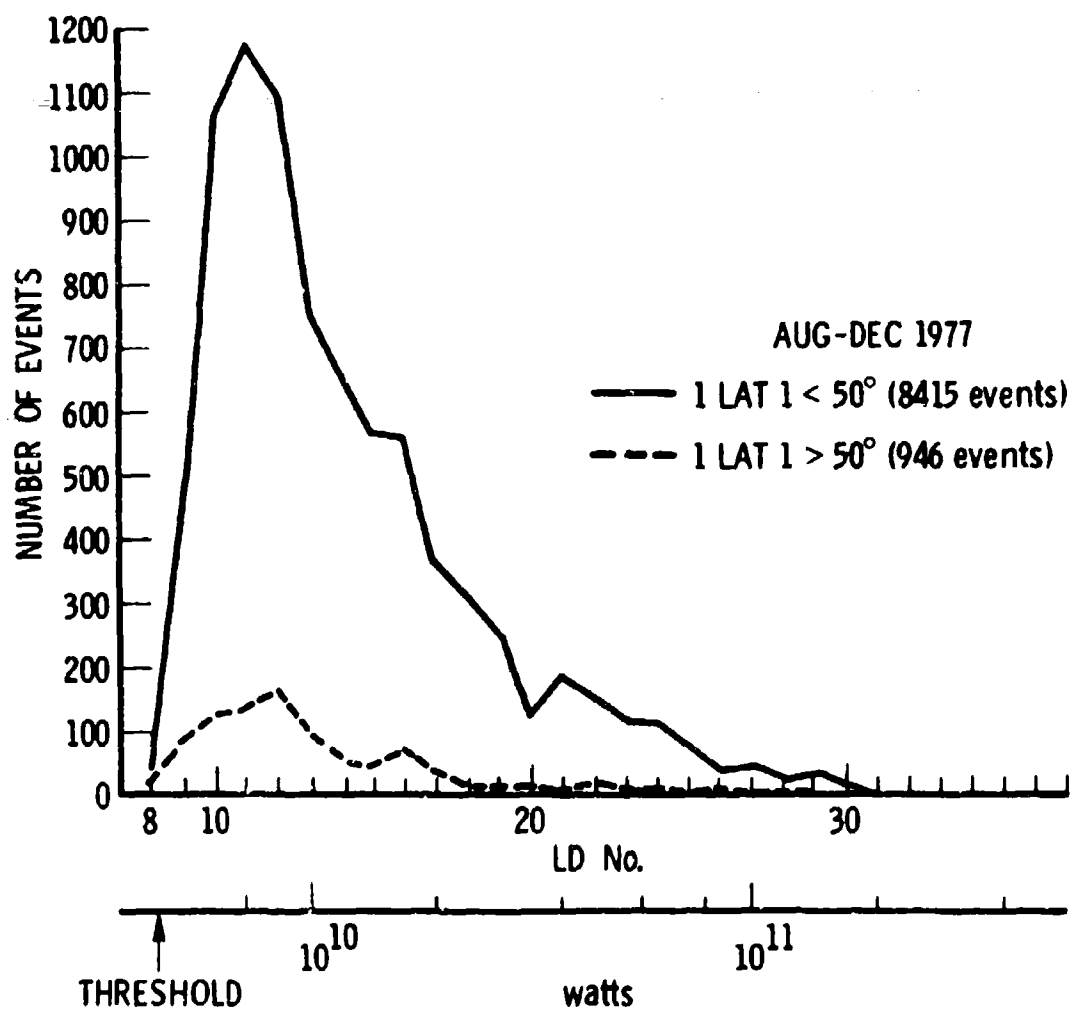


Figure 3b. Distribution of peak optical power for two latitude regions: high latitude and equatorial

Probability of occurrence of peak optical power above the threshold of 4×10^9 watts was also evaluated from the PBE data. As shown by Figure 3a, the median for this distribution is about 10^{10} watts, and somewhat less than 1% of the detected lightning strokes had power in excess of 10^{11} watts. No power larger than 7×10^{11} watts has been observed. The relatively high detection threshold of the PBE sensor severely distorts the true distribution of peak power, since a great deal of all lightning strokes have power below this threshold. A previous DMSP lightning sensor, called the SSL sensor, provided a frequency distribution over the range $10^8 - 10^{10}$ watts (Turman, 1976). Approximately 87% of all lightning flashes in this range had peak power below 4×10^9 watts, and it was estimated that about 40% of all lightning strokes had power below the SSL threshold. Therefore, the PBE sensor, even in its most sensitive sampling rate mode, will detect only about 8% of all lightning flashes occurring within its view.

GEOGRAPHICAL DISTRIBUTION OF LIGHTNING ACTIVITY

One of the primary goals of this project is to measure the geographical distribution of lightning activity. The relatively large field of view of the sensor, however, allows only a coarse-grain development of the distribution. Geographical bins, $10^\circ \times 10^\circ$, were used in sorting the lightning data. From its sun-synchronous, polar orbit, the DMSP satellite sees the earth continuously at local times of dawn (approximately 0700) and dusk (approximately 1900). The orbital period is 100 minutes, and 15 orbits are completed each day. The result is that the satellite subpoint

resides within each of these bins for an average of 1-5 minutes per day for each of the dawn and dusk passes. There are some geographical regions, however, which receive less coverage because of the primary mission operational schedule. Most of these power-down regions were over the Pacific Ocean and Indian Ocean.

Lightning count rate for each of the geographical regions was determined by counting the number of lightning strokes detected while the satellite subpoint was within that region and then dividing by the total time that the subpoint was within that region. Figures 4-6 show the resulting distributions for dawn and dusk time frames for 2 August - 10 September, 11 September - 11 October 1977, and 6 November - 2 December 1977. Nominal sampling period for each of the $10^\circ \times 10^\circ$ bins is 30 minutes.

DISCUSSION

At present, the most authoritative work on lightning activity distribution comes from the World Meteorological Organization (WMO) tabulations of thunderstorm days (WMO Report TP. 21, 1956). These tabulations are based on weather station reports of thunderstorms, and the accuracy of these data are limited by the number and locations of ground observation stations. A limited series of satellite observations from the OSO 2 and OSO 5 satellites have also provided distributions of night-time lightning activity within the latitude bands of $\pm 35^\circ$ (Vorpahl, Sparrow and Ney, 1970, and Sparrow and Ney, 1971).

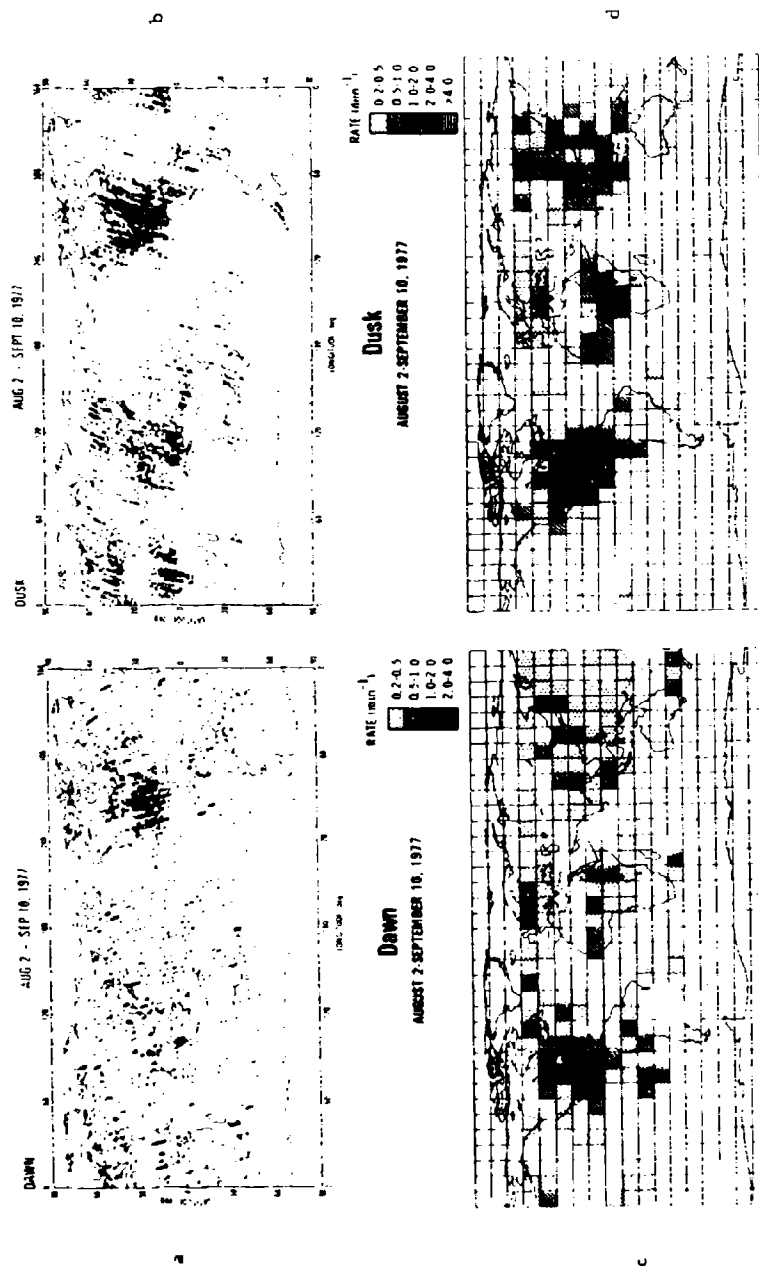


Figure 4. Lightning distribution for the period August 2-September 10, 1977.
a. Distribution at dawn. b. Dusk distribution. c. Occurrence distribution at dawn. d. Occurrence distribution at dusk.

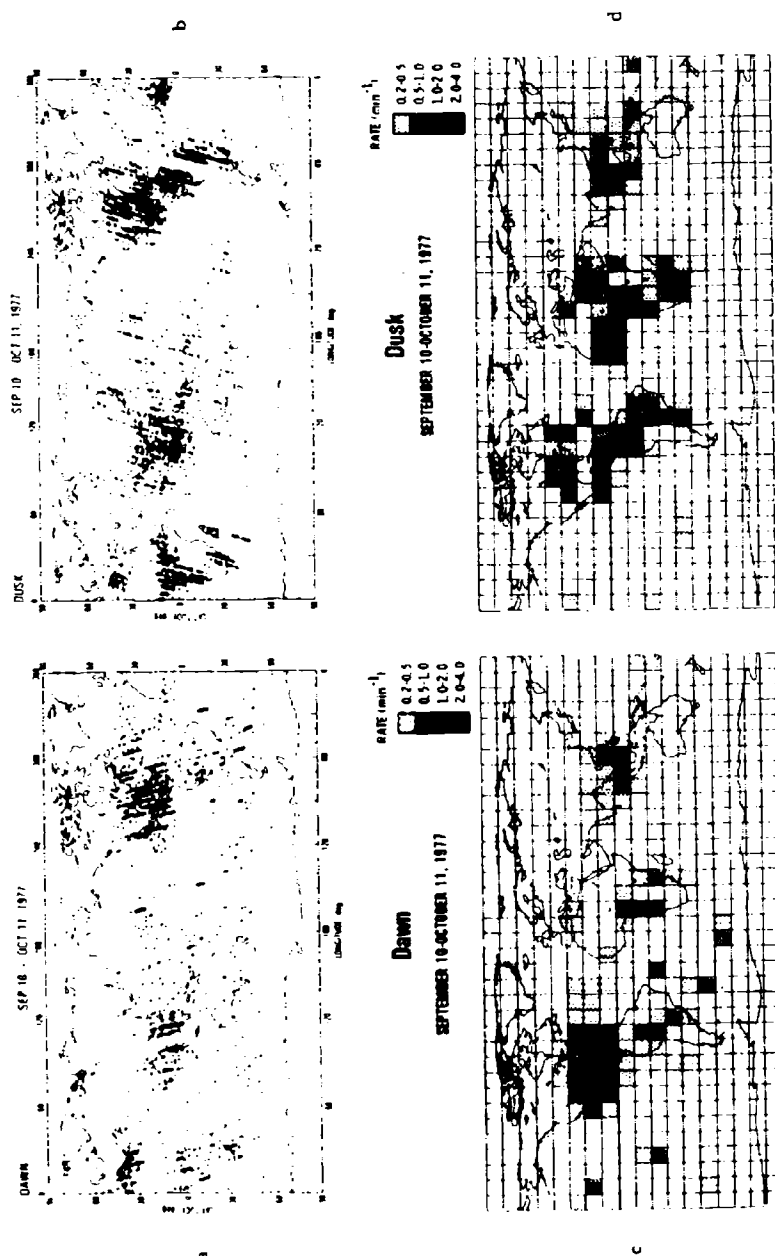


Figure 5. Lightning distribution for the period September 10-October 11, 1977.
a. Distribution of observations for dawn. b. Distribution of observations at dusk. c. Occurrence distribution at dawn. d. Occurrence distribution at dusk.

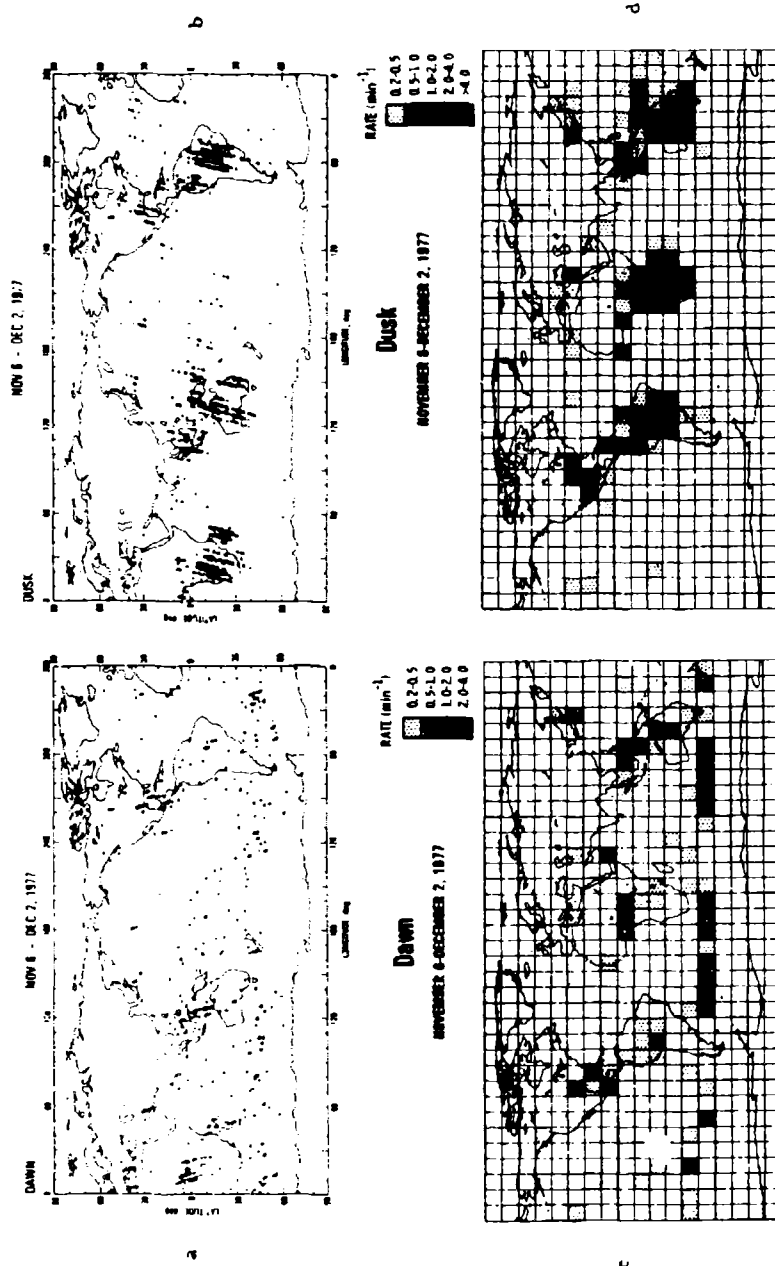


Figure 6. Lightning distribution for the period November 6-December 2, 1977.
 a. Distribution of observations for dawn. b. Distribution of observations for dusk. c. Occurrence distribution for dawn. d. Occurrence distribution for dusk.

The lightning data now available from the PBE experiment allows completely global, unbiased distributions of lightning activity which can be grouped by time (dawn/dusk) and month or season. The first of these distributions are shown in Figures 4-6. Some general trends can be deduced from these results. As would be expected, a definite diurnal trend is displayed over the land masses, with higher lightning activity at dusk as opposed to dawn. The reverse trend is noted over the oceans, with higher activity at dawn. Ocean activity is considerable lower than that over land, but there are a few pockets of significant lightning activity (0.5 - 1.0 per minute) over the oceans. During the Aug-Sep time frame, one such area is off the west coast of South America centered at 10° S, 100° W, and another is in the South Pacific off the east coast of Australia, around 30° S, 170° E. The North Atlantic also has some regions with high level lightning activity. During Sep-Oct, active regions appear in the dawn distribution in the South Pacific (in the vicinity of Tahiti), in the North Pacific (in the vicinity of Hawaii) and in the South Atlantic (Falkland Islands). Most oceanic lightning activity in the dusk distribution is

probably associated with land mass weather, but an interesting region of high activity exists to the east of New Guinea.

The regions of highest lightning activity are easily identified in the distributions, and correspond well with those areas classically regarded as lightning capitols of the world. The August - September distributions show the following high activity areas: (a) Southeast United States, Gulf of Mexico, and Central America (bounded roughly by latitude 10° - 40° N, longitude 80° - 110° W), (b) Central Africa (Zaire and the Congo basin), (c) Southeast Asia (Malaysia, Sumatra, Borneo), (d) India and Southern China. Note that there is little diurnal variation for the Southeast U. S., Gulf of Mexico region, probably because the warm Gulf waters can maintain through the night thunderstorm activity initiated over land regions during the day.

A seasonal change is seen in the September - October distributions. Southern hemisphere activity becomes more prominent, and the strong Gulf of Mexico dusk activity vanishes. High activity regions are: (a) Central United States, (b) Florida and Gulf of Mexico at dawn, (c) Central America, (d) North and Central South America (Columbia, Venezuela, Brazil, Uruguay), (e) Africa (Zaire, Congo Basin, Mozambique, South Africa), and (f) Southeast Asia (Malaysia, Sumatra, Borneo, Thailand, Cambodia and South Viet Nam).

The seasonal shift of lightning activity from the Northern hemisphere to the southern hemisphere during the period August to November follows the shift of the cumulus cloud distribution from also the northern to the southern hemisphere. Figures 7, 8, 9 show the progression of the cumulus



Figure 7. GOES-1 Satellite IR map of the cloud distribution for
August 2, 1977

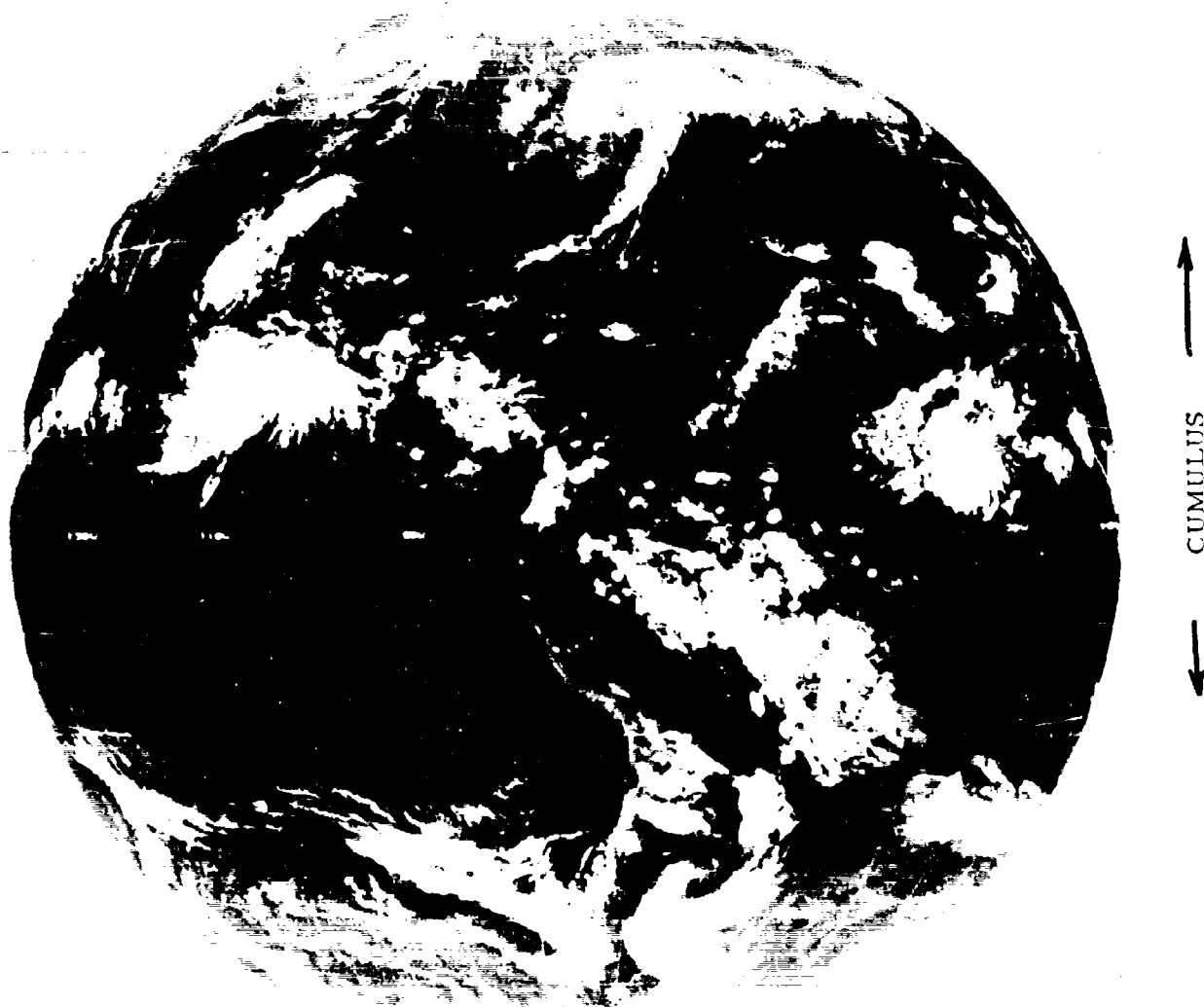


Figure 8. GOES-1 Satellite IR map of the cloud distribution for October 4, 1977

Figure 9. GOES-1 Satellite IR map of the cloud distribution
for November 30, 1977



CUMULUS



Figure 9

clouds (identified by the puffy white spots on the GEOS satellite IR photographs) as they move south. The photos also show clearly the intertropical convergence zone at the equator which usually contains some lightning activity and also the land domination of the cumulus distribution. As one would suspect from ground observations, lightning correlates well with the formation of cumulus clouds.

The average count rate per minute (Table 3) does not seem to change appreciably between dawn and dusk times, nor over the months analyzed to date. The projection of the sensor field of view on the ground is a circle of about 780 Km radius; the sensor therefore observes a surface area of $1.9 \times 10^6 \text{ Km}^2$. The average lightning rate per unit surface area is therefore about $1 \times 10^{-7} \text{ Km}^{-2} \text{ min}^{-1}$. As mentioned earlier, we estimate that the PBE sensor detects only about 8% of all lightning flashes occurring within its viewing area. From these data, then, we estimate that the total lightning flash rate averages about $1.3 \times 10^{-6} \text{ Km}^{-2} \text{ min}^{-1}$. The total worldwide lightning flash rate is then on the order of 600 min^{-1} or on the order of 10 per second. This rate is somewhat lower than the traditionally accepted (and largely untested) value of 100 sec^{-1} (Brooks, 1925).

However, the above estimate of global lightning activity is somewhat misleading, because the satellite passes over many areas of little or no lightning activity. But if the occurrence rates for all of the $10^\circ \times 10^\circ$ bins are summed over the world, only the active areas contribute to this global rate. Table 3 gives the summed rates for the study periods.

TABLE 3

Global Occurrence Rates

	Aug-Sep	Sep-Oct	Nov
Dawn	1.2 sec ⁻¹	1.1 sec ⁻¹	0.6 sec ⁻¹
Dusk	1.6 sec ⁻¹	1.6 sec ⁻¹	1.1 sec ⁻¹

Now if the PBE-2 detector observes only 8% of the lightning flashes in its field of view and one allows another factor of 5-10 for cloud attenuation, the $\sim 2 \text{ sec}^{-1}$ satellite rate agrees quantitatively with the mythical 100 sec^{-1} global rate. However, such calculations are purely speculative until accurate ground-satellite coordinated observations now in progress can be evaluated.

APPLICATIONS

Lightning is a principal contributor to atmospheric radio noise. CCIR (1963) has published contour maps of the global distribution of noise with season and local time. Most of the observing stations for the study were located on continental land masses and thus leave open the question of how good the estimates are over the oceans. The satellite data can explore this question in detail.

Figure 10a shows the high occurrence rates for August plotted on the CCIR maps for June-Aug and the September-October data on the CCIR September-November maps. In Figure 10 the agreement is good for North America, but there is a displacement between noise enhancements in S. E. Asia and Africa, suggesting climate changes over the 15 year span between the CCIR study and our data. The disagreement over South America may be due to lack of satellite coverage which seemed to be prevalent there.

Figure 10b shows very good agreement between the satellite data and the CCIR maps. However Figure 6 shows a dramatic shift of lightning activity to the southern hemisphere which is not reflected by the CCIR

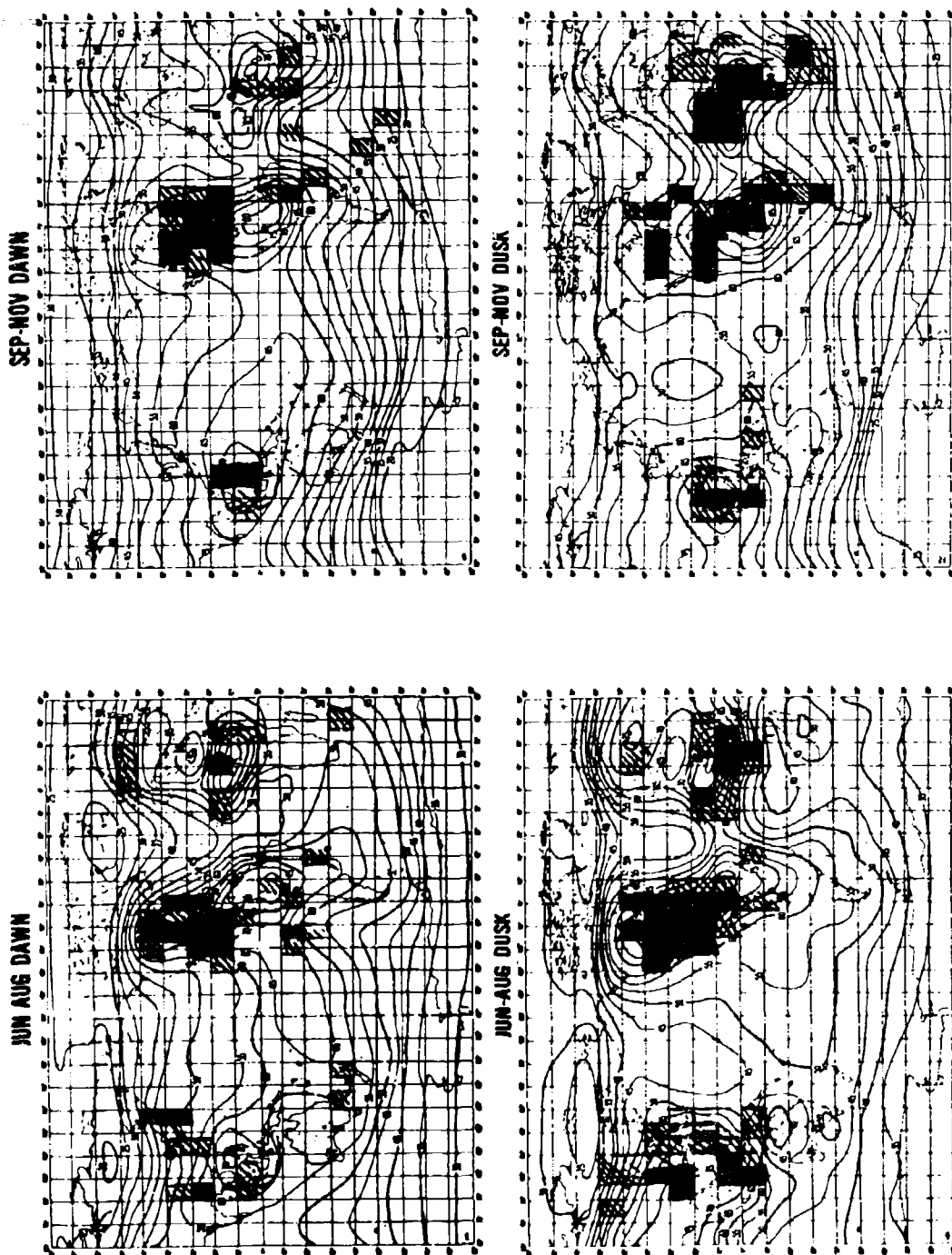


Figure 10. Comparison of CCIR noise map for (a) June-August with the Autst lightning detector data, and (b) September-November with the September-October satellite data. The solid areas represent occurrence rate above 1 min^{-1} .

maps. Thus one would be in error if the CCIR map for September - November were used for November noise predictions. Thus we come to a suggested change for a revision of the CCIR maps: that November be included with December and that the equinox period of September - November be shortened to September - October. There appears to be no justification for increasing the number of observing stations since most of the activity is over land.

CONCLUSIONS

We have shown an initial look at the global distribution of lightning and its seasonal variation. There have been some unexpected results such as the dramatic shift of activity with season, and the ocean activity at dawn. With more study and comparison with ground data, we hope to provide experimenters and theoretical investigators with basic models of lightning occurrence that will enable them to attack new problems in atmospheric and solar-terrestrial relations.

REFERENCES

- Berger, K., Novel observations on lightning discharges, J. Franklin Institute, 283, 478, 1967.
- Brooks, C. E. P., The distribution of thunderstorms over the globe, Geophysical Memoirs, 24, 147, 1925.
- CCIR Report #332, "World distribution and characteristics of atmospheric radio noise," ITU, Geneva, 1964.
- Edgar, B. C., and Turman, B. N., Satellite optical sensing of lightning activity over the S. E. United States, presented at the Fall Meeting of the American Geophysical Union, San Francisco, California, December 1977.
- Sparrow, J. G., and E. P. Ney, Lightning observations by satellite, Nature, 232, 540, 1971.
- Turman, B. N., Analysis of lightning data from the DMSP satellite, Proceedings of the Seventh Conference on Aerospace and Aeronautical Meteorology and Symposium on Remote Sensing from Satellites, p. 188, American Meteorological Society, Boston, Mass. 1976.
- Uman, M. A., Lightning, McGraw-Hill, N. Y., 1969.
- Vorpahl, J., J. G. Sparrow, E. P. Ney, Satellite Observations of Lightning, Science, 169, 860, 1970.
- World Meteorological Organization, Report TP. 21, World distribution of thunderstorm days, Part II, Geneva, 1956.

LABORATORY OPERATIONS

The Laboratory Operations of The Aerospace Corporation is conducting experimental and theoretical investigations necessary for the evaluation and application of scientific advances to new military concepts and systems. Versatility and flexibility have been developed to a high degree by the laboratory personnel in dealing with the many problems encountered in the nation's rapidly developing space and missile systems. Expertise in the latest scientific developments is vital to the accomplishment of tasks related to these problems. The laboratories that contribute to this research are:

Aerophysics Laboratory: Launch and reentry aerodynamics, heat transfer, reentry physics, chemical kinetics, structural mechanics, flight dynamics, atmospheric pollution, and high-power gas lasers.

Chemistry and Physics Laboratory: Atmospheric reactions and atmospheric optics, chemical reactions in polluted atmospheres, chemical reactions of excited species in rocket plumes, chemical thermodynamics, plasma and laser-induced reactions, laser chemistry, propulsion chemistry, space vacuum and radiation effects on materials, lubrication and surface phenomena, photo-sensitive materials and sensors, high precision laser ranging, and the application of physics and chemistry to problems of law enforcement and biomedicine.

Electronics Research Laboratory: Electromagnetic theory, devices, and propagation phenomena, including plasma electromagnetics; quantum electronics, lasers, and electro-optics; communication sciences, applied electronics, semiconducting, superconducting, and crystal device physics, optical and acoustical imaging; atmospheric pollution; millimeter wave and far-infrared technology.

Materials Sciences Laboratory: Development of new materials; metal matrix composites and new forms of carbon; test and evaluation of graphite and ceramics in reentry; spacecraft materials and electronic components in nuclear weapons environment; application of fracture mechanics to stress corrosion and fatigue-induced fractures in structural metals.

Space Sciences Laboratory: Atmospheric and ionospheric physics, radiation from the atmosphere, density and composition of the atmosphere, aurorae and airglow; magnetospheric physics, cosmic rays, generation and propagation of plasma waves in the magnetosphere; solar physics, studies of solar magnetic fields; space astronomy, x-ray astronomy; the effects of nuclear explosions, magnetic storms, and solar activity on the earth's atmosphere, ionosphere, and magnetosphere; the effects of optical, electromagnetic, and particulate radiations in space on space systems.

THE AEROSPACE CORPORATION
El Segundo, California